Mon. Not. R. Astron. Soc. **369,** 89–96 (2006) doi:10.1111/j.1365-2966.2006.10262.x

On searches for gravitational waves from mini-creation events by laser interferometric detectors

B. P. Sarmah,[1,2⋆] S. K. Banerjee,[1,3⋆] S. V. Dhurandhar[1⋆] and J. V. Narlikar[1⋆]

[1]*Inter-University Centre for Astronomy and Astrophysics, Post Bag 4, Ganeshkhind, Pune 411007, India*
[2]*Department of Mathematical Sciences, Tezpur University, Tezpur 784028, India*
[3]*Department of Mathematics, Amity School of Engineering, Sector 125, Noida 201301, India*

Accepted 2006 February 27. Received 2006 February 22; in original form 2005 September 20

ABSTRACT

As an alternative view to the standard big bang cosmology, the quasi-steady-state cosmology argues that the Universe was not created in a single great explosion: it did not have a beginning, nor will it ever come to an end. The creation of new matter in the Universe is a regular feature occurring through finite explosive events. Each creation event is called a mini-bang, or a mini-creation event. Gravitational waves are expected to be generated as a result of any anisotropy present in this process of creation. A mini-creation event that ejects matter in two oppositely directed jets is thus a source of gravitational waves, which can in principle be detected by laser interferometric detectors. In the present work we consider the gravitational waveforms propagated by linear jets and then estimate the response of laser interferometric detectors such as LIGO and LISA.

Key words: gravitational waves – cosmology: theory.

1 INTRODUCTION

The quasi-steady-state cosmology (QSSC) was proposed and explored in a series of papers by Hoyle, Burbidge & Narlikar (1993, 1994a,b, 1995) as a possible alternative to the standard big bang cosmology. The QSSC is based on a Machian theory of gravity that satisfies the Weyl postulate and the cosmological principle. The effective field equations are Einstein's equations of general relativity together with a negative cosmological constant and a trace-free zero-mass scalar field, yielding a wide range of solutions for the spatial sections of zero, positive and negative curvatures (Sachs, Narlikar & Hoyle 1996).

Instead of a single initial infinite explosion called the big bang, the QSSC has a universe without a beginning, and its dynamical behaviour is sustained by an endless chain of mini-bangs, better known as mini-creation events (MCEs) randomly distributed over space. The universe itself has a long-term de-Sitter-type expansion with a characteristic time-scale of $\sim 10^{12}$ yr, along with short-term oscillations of period $\sim$50 Gyr. The oscillations respond in phase to 'on–off' creation activity in MCEs, with matter being created only in strong gravitational fields associated with dense aggregates of matter. The typical MCE may explain the outpouring of matter and radiation from a wide range of extragalactic objects of varying sizes ranging from supercluster-size mass, $\sim 10^{16}\,\mathrm{M}_{\odot}$, to masses of the order of 10^{6}–$10^{13}\,\mathrm{M}_{\odot}$ (Hoyle et al. 1993). The cosmology has offered alternative interpretations of phenomena such as the microwave background, abundances of light nuclei, the m–z relation of high-redshift supernovae, etc. (Hoyle, Burbidge & Narlikar 2000; Narlikar, Vishwakarma & Burbidge 2002). It has also suggested tests to distinguish it from the standard model (Narlikar & Padmanabhan 2001). One such possibility is provided by gravitational-wave astronomy.

Gravitational waves are expected to be generated if anisotropy is present in an MCE. Das Gupta & Narlikar (1993) performed a preliminary calculation relating the size and anisotropy of a typical MCE to the feasibility of its being detected by LIGO-type detectors. Here we carry out a more refined study of MCEs in which matter is ejected more like a jet. We must have a realistic model of the detector noise $n(t)$ to decide what information could be extracted from gravitational waveforms. This noise might have both Gaussian and non-Gaussian components but we will restrict ourselves to the statistical errors arising from Gaussian noise only. We can describe the remaining Gaussian noise by its spectral density $S_{\mathrm{n}}(f)$, where f is the frequency. The form of $S_{\mathrm{n}}(f)$ of course depends on the parameters of the detector.

We first consider the cosmogony of the creation process that leads to the creation and ejection of matter. We show why the creation phenomenon may have a non-isotropic character, with ejection taking place along preferred directions. To measure its gravitational-wave effect we calculate the gravitational amplitude generated by an MCE of mass M at a cosmological distance r, and then compare the signal-to-noise ratio detectable by the ground-based laser interferometric detectors of the LIGO (Laser Interferometric Gravitional Wave Observatory) and the advanced LIGO type within the frequency range

⋆E-mail: bhim@tezu.ernet.in (BPS); skb@iucaa.ernet.in (SKB); sanjeev@iucaa.ernet.in (SVD); jvn@iucaa.ernet.in (JVN)

10 to 1000 Hz with the signal-to-noise ratio detectable by the Laser Interferometric Space Antenna (LISA) within the frequency range 10^{-4} to 10^{-1} Hz.

2 MATTER CREATION IN THE QSSC

The creation of matter in the QSSC proceeds via an exchange of energy from a background reservoir of a scalar field C of negative energy and stresses. The details of the process have been described in Hoyle et al. (2000) and papers on QSSC such as Hoyle et al. (1995a) and Sachs et al. (1996). We outline here the relevant aspects of the process that concerns us.

First, the basic particle to be created is the so-called Planck particle, which has mass

$$m_{\rm p} = \sqrt{\frac{3\hbar c}{4\pi G}}. \tag{1}$$

This particle itself is unstable on a time-scale of 10^{-43} s. It subsequently decays into baryons through a series of processes that are currently discussed in the GUTs $\rightarrow$ quark gluon plasma $\rightarrow$ baryons in high-energy particle physics. However, it is the initial stage of this sequence of events that concerns us here, viz. the location of creation of Planck particles. Can creation take place anywhere? The answer is 'no'. The process requires a high enough energy threshold of the C field:

$$C_i C^i = m_{\rm p}^2 c^4, \tag{2}$$

where $C_i = \partial C/\partial x^i$, x^i ($i = 0, 1, 2, 3$, x^0 time-like) being the space–time coordinates.

The normal cosmological background of the C field is below this threshold. Had the universe been homogeneous, there would have been no creation of matter. However, the real Universe, although smooth and homogeneous on a large-enough scale (so that it can be described by the Robertson–Walker line element), has pockets of strong gravitational field, such as occur in the neighbourhood of collapsed massive objects, often dignified by the name 'black holes'.

We shall use the name 'near black hole' (NBH) to denote a collapsed massive object whose size would be very slightly in excess of that of its event horizon, *if it were a Schwarzschild black hole*. Thus a spherical object of mass M would have a radius

$$r_0 = \frac{2GM}{c^2} + \epsilon, \quad \epsilon \ll r_0. \tag{3}$$

In the neighbourhood of such an object, at a distance r from its centre,

$$C_i C^i = \frac{{m_c}^2}{1 - (2GM/c^2 r)}, \quad r > r_0, \tag{4}$$

where $m_c (< m_{\rm p})$ is the background level of the C-field energy density. It is thus possible that at r sufficiently close to r_0, the value of $C_i C^i$ crosses the creation threshold. This is when creation of matter would take place. Furthermore, because the creation of matter is accompanied by the creation of the C field, the latter generates negative stresses close to $r = r_0$, which blow the created matter outwards.

In the above example the creation is isotropic, and the resulting disturbances will not generate gravitational waves. This situation is, however, highly idealized. The real massive object will not be spherically symmetric, nor will the creation and expulsion of new matter from it be isotropic about its centre.

Even the next stage of asymmetry is sufficient to generate gravitational waves, namely that of a spinning collapsed massive object that is idealized as the Kerr black hole. The line element of the external space–time for such a black hole is given by

$$\begin{aligned} {\rm d}s^2 = {} & \frac{\Delta}{\Sigma}({\rm d}t - h\sin^2\theta\,{\rm d}\phi)^2 - \frac{\sin^2\theta}{\Sigma}[(r^2 + h^2)\,{\rm d}\phi - h\,{\rm d}t]^2 \\ & - \frac{\Sigma}{\Delta}\,{\rm d}r^2 - \Sigma\,{\rm d}\theta^2, \end{aligned} \tag{5}$$

where

$$\Delta \equiv r^2 - 2mr + h^2, \quad \Sigma \equiv r^2 + h^2\cos^2\theta, \tag{6}$$

and $m = MG/c^2$, $h = J/Mc$, where M and J are respectively the mass and angular momentum of the black hole. The Kerr black hole has an outer horizon at

$$r_+ = m + \sqrt{m^2 - h^2}, \tag{7}$$

while the surface of revolution, given by

$$r_{\rm s}(\theta) = m + \sqrt{m^2 - h^2\cos^2\theta}, \tag{8}$$

is called the static limit. Between r_+ and $r_{\rm s}$ is the region known as the ergosphere, wherein matter is made to rotate in the same direction as the spinning black hole.

As in the case of the Schwarzschild black hole, the spinning collapsed massive object here will simulate a NBH with spin, and its exterior solution will be approximately given by the above equation (7). Here too we expect $C_i C^i$ to be raised above the threshold close to the horizon, because it is given by

$$C_i C^i = \frac{[(r^2 + h^2)(r^2 + h^2\cos^2\theta) + 2mrh^2\sin^2\theta]}{(r^2 + h^2\cos^2\theta)(r^2 - 2mr + h^2)}. \tag{9}$$

It can be seen that the above expression is maximum at the poles ($\theta = 0, \pi$) and minimum at the equator ($\theta = \pi/2$). Thus the creation threshold will be attained more easily at the poles than at the equator, leading to preferential creation of matter there. However, because of the property of the ergosphere of dragging any matter along with the spinning mass, only matter created near the polar regions ($\theta = 0, \pi$) will find its way out as it is ejected by the C field. In other words, we expect created matter to find its way out along the polar directions in the form of oppositely directed jets. This is the canonical source of gravitational waves in the QSSC.

A word of caution is needed in regards to the above argument. We have assumed that, in the neighbourhood of a typical NBH, the strength of the cosmological C field will be small. Thus we have assumed that the Schwarzschild and Kerr solutions are not significantly modified by the C field. This assumption can be checked only by obtaining an exact solution of a NBH with the C field. We have not carried out this (rather difficult, possibly impossible) exercise, but have relied on approximations based on series expansions. In any case, for the purpose of this paper we have given a rationale for expecting the simplest cosmological sources of gravitational waves to be twin-jet systems spewing out newly created matter linearly in opposite directions.

3 GRAVITATIONAL RADIATION FROM AN MCE

In the QSSC the created matter near a Kerr-like black hole moves rapidly along the polar directions in the form of oppositely directed jets. Such an object is endowed with a changing quadrupole moment, causing the system to emit gravitational waves. In the following we estimate its amplitude.

We set up a spherical polar coordinate system in which the jet is expanding linearly with a speed u in the ϵ–ψ direction, and consider the z-direction to be the line of sight. The gravitational-wave amplitude under the quadrupole approximation (a good approximation for a very long distance source) can be calculated from the reduced-mass quadrupole moment of the source. The reduced-mass quadrupole moment of a source is given by

$$Q_{ij} = \int_V \rho \mathrm{d}V \left(r_i r_j - \frac{1}{3}\delta_{ij} r^2 \right), \tag{10}$$

where ρ is the mass per unit volume. We assume that away from the NBH the geometry is almost Euclidean.

The components of the gravitational-wave amplitude at the detector at time t are given by

$$\bar{h}_{ij} = \frac{2G}{c^4 R} \left[\ddot{Q}_{ij} \left(t - \frac{R}{c} \right) \right], \tag{11}$$

where R is the radial distance of the object from the detector. At the source we have the time $t_0 = t - R/c$. The transverse traceless components can be extracted from $\bar{h}_{ij}$ through the projection operator $P^b_a = \delta^b_a - n^b n_a$ as

$$\bar{h}^{\mathrm{TT}}_{ij} = P^k_i P^l_j \bar{h}_{kl} - \frac{1}{2} P_{ij} \left(P^{kl} \bar{h}_{kl} \right). \tag{12}$$

For gravitational waves propagating along the z-direction, $n_a = (0, 0, 1)$, the '+' and the '×' polarization components of the wave are

$$h_+ = \frac{\bar{h}_{11} - \bar{h}_{22}}{2} \quad \text{and} \quad h_\times = \bar{h}_{12}. \tag{13}$$

We will assume the radial velocity of the jet to be u, so that $|ut_0| \ll R$.

For a time t_0 typical of the source, the three spatial coordinates are $r_1 = ut_0 \sin\epsilon \cos\psi$, $r_2 = ut_0 \sin\epsilon \sin\psi$ and $r_3 = ut_0 \cos\epsilon$. The non-vanishing components of the symmetric mass quadrupole moment (Q_{ij}) tensor are

$$\begin{aligned}
Q_{11} &= \frac{2Q_0}{3} \left(\sin^2\epsilon \, \cos^2\psi - \frac{1}{3} \right), \\
Q_{12} &= \frac{Q_0}{3} \sin^2\epsilon \, \sin 2\psi, \\
Q_{13} &= \frac{Q_0}{3} \sin 2\epsilon \, \cos\psi, \\
Q_{22} &= \frac{2Q_0}{3} \left(\sin^2\epsilon \, \sin^2\psi - \frac{1}{3} \right), \\
Q_{23} &= \frac{Q_0}{3} \sin 2\epsilon \, \sin\psi, \\
Q_{33} &= \frac{2Q_0}{3} \left(\cos^2\epsilon - \frac{1}{3} \right),
\end{aligned} \tag{14}$$

where $Q_0 = \dot{M} u^2 t_0^3$. The mass creation rate is $\dot{M} = A\rho u$, where A is the area of the jet.

The two polarization components can be calculated as

$$\begin{aligned}
h_+(t_0) &= h_{\mathrm{char}} \, \sin^2\epsilon \, \cos 2\psi, \\
h_\times(t_0) &= h_{\mathrm{char}} \, \sin^2\epsilon \, \sin 2\psi,
\end{aligned} \tag{15}$$

where

$$h_{\mathrm{char}} = \frac{4G\rho A u^3 t_0}{c^4 R} = \frac{4G\dot{M} u^2 t_0}{c^4 R}$$

$$\sim 2.7 \times 10^{-17} \left(\frac{\dot{M}}{200\,\mathrm{M}_\odot\,\mathrm{s}^{-1}} \right) \left(\frac{u}{0.8c} \right)^2 \times \left(\frac{t_0}{1000\,\mathrm{s}} \right) \left(\frac{R}{3\,\mathrm{Gpc}} \right)^{-1}. \tag{16}$$

The MCE sweeps over the band of the detector from high to low frequency. For LISA the low end of the band is taken to be 10^{-4} Hz, which corresponds to about 10^4 s ∼ a few hours. In this period the LISA hardly changes orientation. Assuming a random distribution and orientations of the MCEs, we perform appropriate averages over the directions and orientations of the MCEs.

The angle-averaging of a quantity V is performed according to

$$\langle V \rangle_\psi = \left[\frac{1}{2\pi} \int_0^{2\pi} V^2 \mathrm{d}\psi \right]^{1/2},$$

$$\langle V \rangle_\epsilon = \left[\frac{1}{2} \int_0^{\pi} V^2 \sin\epsilon \mathrm{d}\epsilon \right]^{1/2},$$

$$\langle V \rangle_{\epsilon,\psi} = \left[\frac{1}{4\pi} \int_{\psi=0}^{2\pi} \int_{\epsilon=0}^{\pi} V^2 \sin\epsilon \mathrm{d}\epsilon \mathrm{d}\psi \right]^{1/2}.$$

Thus,

$$\begin{aligned}
\langle h_+(t_0) \rangle_\psi &= \langle h_\times(t_0) \rangle_\psi = \frac{1}{\sqrt{2}} \, h_{\mathrm{char}} \, \sin^2\epsilon, \\
\langle h_+(t_0) \rangle_{\epsilon,\psi} &= \langle h_\times(t_0) \rangle_{\epsilon,\psi} = \frac{2}{\sqrt{15}} \, h_{\mathrm{char}}.
\end{aligned} \tag{17}$$

Before proceeding further we look at the overall stability of the system under the energy loss suffered through gravitational waves. An order-of-magnitude calculation indicates that the situation is as follows.

The rate of emission of gravitational waves corresponding to (16) above is given by

$$P_{\mathrm{GW}} \cong \frac{c^3}{16\pi G} \alpha \left(\frac{4G\dot{M}u^2}{c^4 R} \right)^2 4\pi R^2, \tag{18}$$

where α is a dimensionless constant of order unity (see, for example, Misner, Thorne & Wheeler 1973, pp. 975–1005). We compare this with the rate of addition of kinetic energy to the system,

$$P_{\mathrm{KE}} \cong \frac{1}{2} \dot{M} u^2. \tag{19}$$

If this ratio $P_{\mathrm{GW}} : P_{\mathrm{KE}}$ is small compared with unity, the radiation reaction will not slow down the source significantly. From (18) and (19) we obtain

$$\eta = \frac{P_{\mathrm{GW}}}{P_{\mathrm{KE}}} \cong \frac{8\alpha G\dot{M}u^2}{c^5} = 8\alpha \frac{G\dot{M}}{c^3} \beta^2, \tag{20}$$

where $u = \beta c$. (Although we have taken $\beta = 0.8$ as a typical example, the above Newtonian calculation will be within an order of magnitude of the relativistic one.)

For $\dot{M} = 200\,\mathrm{M}_\odot\,\mathrm{s}^{-1}$ and $\alpha \sim 1$, we have $\eta \sim 5 \times 10^{-3}$. In short, from this simple-minded calculation the kinetic energy created in the source well exceeds the energy radiated away. So by this argument we do not expect the source dynamics to be affected by the radiation process. However, a more detailed computation is required to determine the effect of radiation reaction. This we do not perform here, because our goal in this investigation is to obtain only order-of-magnitude results.

Another aspect of the solution is whether the quadrupole moment formula used in (10) is sufficient to describe the scenario adequately. Had the speed of the jet been small compared with c, i.e. $\beta \ll 1$, we would have been certain of this. In the present case we have taken $\beta \sim 0.8$, and so the implications need more careful attention. It should be noted in this case that higher-order terms are extremely complex to calculate. Given the approximate nature of our source geometry such an exercise is not worth the effort. As we are, at this stage, interested in evaluating the order of magnitude of the overall effect we can argue as follows. For each extra order, the magnitude of the contribution is reduced by a factor β. Thus multipoles of higher order would contribute terms of order β, β^2, β^3, etc., which do not significantly modify the estimate given by the first (quadrupole) term.

4 FOURIER TRANSFORM OF THE GRAVITATIONAL-WAVE AMPLITUDE

The two polarizations of gravitational-wave amplitude that we found in the earlier section have to be expressed in the limited frequency space within which the detector is supposed to be most sensitive. We also redefine our zero of time as the instant at which the gravitational radiation first hits the observer.

The Fourier transforms of $h_+(t_0)$ and $h_\times(t_0)$ are given by

$$\tilde{h}_+(f) = \int_{-\infty}^{\infty} h_+(t_0)\, \exp(-2\pi i f t_0)\, \mathrm{d}t_0 = \frac{\dot{M}Gu^2}{\pi^2 c^4 R}\frac{1}{f^2}\, \sin^2\epsilon\, \cos 2\psi. \quad (21)$$

$$\tilde{h}_\times(f) = \int_{-\infty}^{\infty} h_\times(t_0)\, \exp(-2\pi i f t_0)\, \mathrm{d}t_0 = \frac{\dot{M}Gu^2}{\pi^2 c^4 R}\frac{1}{f^2}\, \sin^2\epsilon\, \sin 2\psi. \quad (22)$$

Plots of $\tilde{h}_+(f)$ and $\tilde{h}_\times(f)$ are shown in Fig. 1. Because the frequency f appears in the denominators of the above expressions, the amplitude of the jet falls in inverse-square fashion as it expands. This causes most of the wave energy to be concentrated in the low-frequency bin. It is thus worthwhile to analyse the detectability of such a wave through a low-frequency detector such as LISA. We will also compare the results with the magnitude detectable by a high-frequency detector such as LIGO.

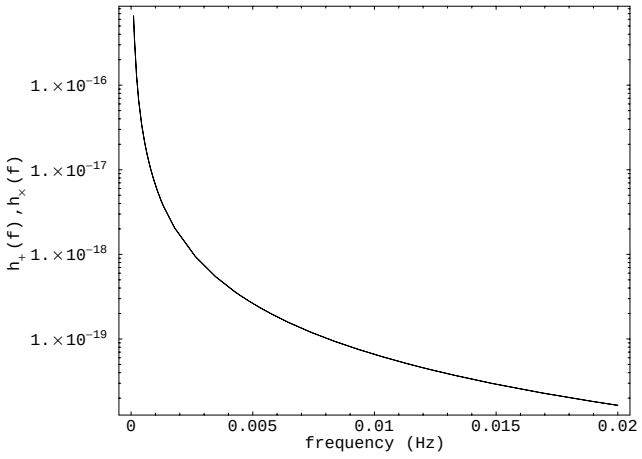

Figure 1. The Fourier transform of the two polarizations of the wave in units of Hz^{-1} are plotted here as a function of frequency for a MCE jet with $\dot{M} = 200\,\mathrm{M}_\odot\,\mathrm{s}^{-1}$, $R = c/2H_0$ (for $h_0 = 0.65$), and $u = 0.8\,c$. Here $\epsilon \sim 15^0$ and ψ is averaged over uniformly. The two components thus averaged are of the same amplitude and hence they overlap.

The $1/f^2$ dependence might suggest infrared divergence of this formula as $f \to 0$. However, the assumed geometry and lifetime of expansion of the source is finite, i.e. t_0 is bounded above. At the relativistic speed assumed here, the source would attain a size of $\sim$200 kpc in a time of $\sim 10^6$ yr. If the source slows down, the time-scale may be longer, typically $\sim 10^8$ yr. Thus instead of $f \to 0$ we have f bounded below, and no divergence arises.

5 DETECTABILITY OF MCES BY LISA

5.1 Time-delay interferometry of LISA

LISA, the laser interferometric space antenna, is a proposed mission that will use coherent laser beams exchanged between three identical spacecraft forming a giant equilateral triangle with each side 5×10^6 km to observe and detect low-frequency gravitational waves from cosmic sources.

In LISA, six data streams arise from the exchange of laser beams between the three spacecraft. The sensitivity of LISA crucially depends on the cancellation of the laser-frequency noise. Because of the impossibility of achieving equal distances between the spacecraft, however, the laser frequency cannot be exactly cancelled. Several schemes have been proposed to combine the recorded data with suitable time delays corresponding to the three arm lengths of the giant triangular interferometer. The idea of time-delayed data combination scheme was proposed by the Jet Propulsion Laboratory team (Armstrong, Eastabrook & Tinto 1999; Tinto & Armstrong 1999; Eastabrook, Tinto & Armstrong 2000). Dhurandhar, Nayak & Vinet (2002) adopted an algebraic approach to this problem of introducing time delays to cancel the laser-frequency noise based on the modules over polynomial rings.

The data combinations that cancel the laser-frequency noise consist of six suitably delayed data streams, the delays being integer multiples of the light travel times between spacecraft, which can be conveniently expressed in terms of polynomials in the three delay operators E_1, E_2, E_3 corresponding to the light travel times along the three arms. The laser-noise cancellation condition puts three constraints on the six polynomials of the delay operators corresponding to the six data streams. The problem therefore consists of finding six-tuples of polynomials that satisfy the laser-noise cancellation constraints. These polynomial tuples form a module, called the *module of syzygies*.

Given any elementary data streams U^i, V^i, a general data combination is a linear combination of these elementary data streams:

$$X(t) = \sum_{i=1}^{3} p_i V^i(t) + q_i U^i(t), \quad (23)$$

where p_i and q_i are polynomials in the time-delay operators E_i, $i = 1, 2, 3$. Thus any data combination can be expressed as a six-tuple polynomial 'vector' (p_i, q_i). For cancellation of laser-frequency noise, only the polynomial vectors satisfying this constraint are allowed, and they form the module of syzygies mentioned above. While the laser-frequency noise and optical bench motion noise can be cancelled by taking appropriate combinations of the beams in the module of syzygies, the acceleration noise of the proof masses and the shot noise cannot be cancelled out in the scheme. These then form the bulk of the noise spectrum. The noise

power spectral density is also expressible in terms of the noise-cancelling polynomials of the time-delay operators. The expression for the noise spectrum will depend on the particular combination of polynomials used.

In our analysis we use the Michelson combination to calculate the response and the noise power spectral density. As shown in Nayak et al. (2003), the Michelson combination has on average almost as good a sensitivity as the optimized combinations. Because we are interested here in order-of-magnitude estimates, the Michelson combination is good enough for our purposes. Moreover, it is easier to calculate relevant quantities for the Michelson combination than for other combinations.

5.2 Estimation of the signal-to-noise ratio of jets in LISA

We choose a coordinate system in which the LISA configuration is at rest and let the x-axis of the coordinate system be perpendicular to one of the LISA arm unit vectors ($\hat{\boldsymbol{n}}_1, \hat{\boldsymbol{n}}_2, \hat{\boldsymbol{n}}_3$). The z-axis is considered perpendicular to the plane of the *LISA* triangle. The unit vector $\hat{\boldsymbol{w}}$ connecting the origin and the source is parametrized by the source angular location (θ, ϕ), so that

$$\hat{\boldsymbol{w}} = \begin{pmatrix} \sin\theta\cos\phi \\ \sin\theta\sin\phi \\ \cos\theta \end{pmatrix}, \tag{24}$$

and the transverse plane is spanned by the unit transverse vectors $\hat{\boldsymbol{\theta}}$ and $\hat{\boldsymbol{\phi}}$, defined by

$$\hat{\boldsymbol{\theta}} = \frac{\partial\hat{\boldsymbol{w}}}{\partial\theta}, \qquad \hat{\boldsymbol{\phi}} = \frac{1}{\sin\theta}\frac{\partial\hat{\boldsymbol{w}}}{\partial\phi}. \tag{25}$$

For the Michelson combination we have the following expressions for the polynomials:

$$\begin{aligned} p_i &= \left\{1 - E_2^2,\, 0,\, E_2\left(E_3^2 - 1\right)\right\}, \\ q_i &= \left\{1 - E_3^2,\, E_3\left(E_2^2 - 1\right),\, 0\right\}. \end{aligned} \tag{26}$$

In the Fourier domain, $E_i = \mathrm{e}^{\mathrm{i}\Omega L_\mathrm{i}}$, where $\Omega = 2\pi f$ is the angular frequency. The *LISA* arm vectors are given by $\boldsymbol{r}_i = L_i\hat{\boldsymbol{n}}_i$ ($i = 1, 2, 3$). However, for the purpose of calculation of the noise and response it is sufficient to consider all the L_i to be equal, to L say.

The noise power spectral density as given by Bender et al. (2000) for this combination is

$$S_\mathrm{M} = 16\, S_\mathrm{shot}\, \sin^2 2\pi f L + S_\mathrm{proof}(32\sin^2 2\pi f L + 8\sin^2 4\pi f L), \tag{27}$$

where

$$S_\mathrm{shot} = 5.3\times10^{-38} f^2\,\mathrm{Hz}^{-1},$$

$$S_\mathrm{proof} = 2.5\times10^{-48} f^{-2}\,\mathrm{Hz}^{-1}.$$

A plot of the noise power density S_M for the Michelson combination is shown in Fig. 2. Several sets of generators have been listed in Dhurandhar et al. (2002). The response of LISA to a source is expressible for a given data combination X in terms of its elementary data stream U^i, V^i as follows:

$$\begin{aligned} \mathcal{R}_X(\Omega;\theta,\phi,\epsilon,\psi) = {} & \tilde{h}_+(\Omega;\epsilon,\psi)F_+(\Omega;\theta,\phi) \\ & +\tilde{h}_\times(\Omega;\epsilon,\psi)F_\times(\Omega;\theta,\phi), \end{aligned} \tag{28}$$

where $F_{+,\times}(\Omega)$ are transfer functions that correspond to the combination X. These are functions of the source angular location and the frequency. For different noise cancelling combinations (U_i, V_i),

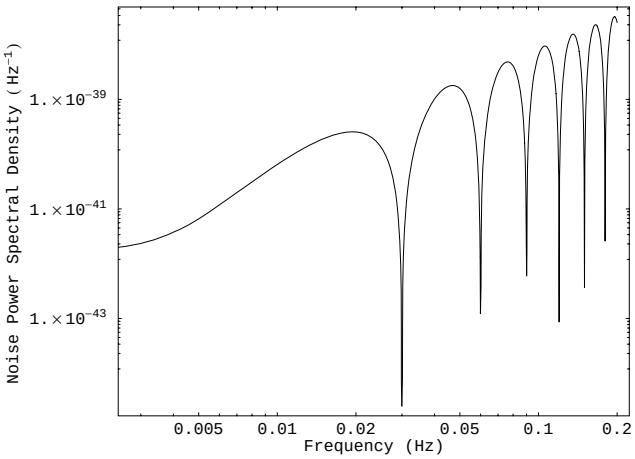

Figure 2. Noise power spectral density S_M for the Michelson combination, as a function of frequency.

$F_{+,\times}(\Omega)$ will have different expressions. Below are quantities for U_1, V_1 (the others are obtained by cyclic permutations):

$$\begin{aligned} F_{U_1;+,\times} &= \frac{\mathrm{e}^{\mathrm{i}\Omega(\hat{\boldsymbol{w}}\cdot\boldsymbol{r}_3+L_2)}}{2(1+\hat{\boldsymbol{w}}\cdot\hat{\boldsymbol{n}}_2)}\left[1-\mathrm{e}^{-\mathrm{i}\Omega L_2(1+\hat{\boldsymbol{w}}\cdot\hat{\boldsymbol{n}}_2)}\right]\xi_{2;+,\times}, \\ F_{V_1;+,\times} &= -\frac{\mathrm{e}^{\mathrm{i}\Omega(\hat{\boldsymbol{w}}\cdot\boldsymbol{r}_2+L_3)}}{2(1-\hat{\boldsymbol{w}}\cdot\hat{\boldsymbol{n}}_3)}\left[1-\mathrm{e}^{-\mathrm{i}\Omega L_3(1-\hat{\boldsymbol{w}}\cdot\hat{\boldsymbol{n}}_3)}\right]\xi_{3;+,\times}, \end{aligned} \tag{29}$$

where

$$\begin{aligned} \xi_{i;+} &= (\hat{\boldsymbol{\theta}}\cdot\hat{\boldsymbol{n}}_i)^2 - (\hat{\boldsymbol{\phi}}\cdot\hat{\boldsymbol{n}}_i)^2, \\ \xi_{i;\times} &= 2(\hat{\boldsymbol{\theta}}\cdot\hat{\boldsymbol{n}}_i)(\hat{\boldsymbol{\phi}}\cdot\hat{\boldsymbol{n}}_i). \end{aligned} \tag{30}$$

In the above, L_i are the arm lengths of LISA ($i = 1, 2, 3$), $\hat{\boldsymbol{w}}$ is the unit vector along the line of sight, and $\hat{\boldsymbol{\theta}}$ and $\hat{\boldsymbol{\phi}}$ are the unit vectors transverse to the line of sight.

The response of LISA to the Michelson combination is given by

$$\mathcal{R}_\mathrm{M} = \sum_{i=1}^{3}[p_i(F_{Vi;+}h_+ + F_{Vi;\times}h_\times) + q_i(F_{Ui;+}h_+ + F_{Ui;\times}h_\times)], \tag{31}$$

where the polynomial functions p_i and q_i are for the Michelson combination given in equation (26). The signal-to-noise ratio corresponding to a particular frequency, say f, is given by

$$\mathrm{SNR}_f = \frac{|\mathcal{R}_\mathrm{M}|}{\sqrt{S_\mathrm{M}}}. \tag{32}$$

The integrated signal-to-noise ratio is then given by

$$\mathrm{SNR} = \left[2\int_0^\infty \frac{|\mathcal{R}_\mathrm{M}|^2}{S_\mathrm{M}}\,\mathrm{d}f\right]^{1/2}. \tag{33}$$

The response $\mathcal{R}_\mathrm{M}$ is now a function of $\epsilon, \psi, \theta, \phi$ and the frequency f. Since the detector is omnidirectional, it will pick up all such sources of various orientations and frequencies in its response. It is therefore necessary to average the response over the orientations of the source and the detector. The expression for the integrated signal-to-noise ratio takes care of the frequency averaging.

We apply this model to a superluminal jet beaming towards us at an angle of nearly 15° from a distance of about half the Hubble distance and with a speed of nearly 80 per cent of the speed of light in vacuum; that is, in this case, $u = 0.8c, \epsilon = 15^\circ, R = c/2H_0$ (for $h_0 = 0.65$).

A plot of the response $\mathcal{R}_\mathrm{M}$ of *LISA* for the Michelson combination is shown in Fig. 3. We have implemented the response function

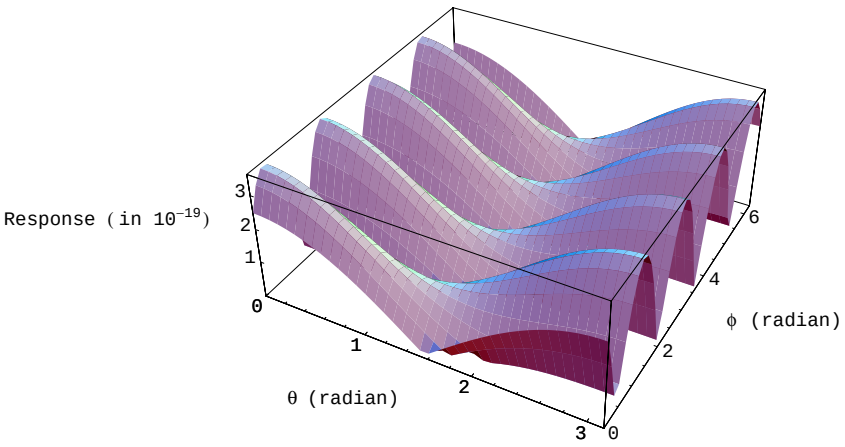

Figure 3. Response $\mathcal{R}_{\rm M}$ of LISA to the jet source at $f = 1$ mHz as a function of the angular location (θ, ϕ) of the source for the Michelson combination.

given by Dhurandhar et al. (2002) and their proper angle averaging, and calculated the signal-to-noise ratio as a function of frequency and the integrated signal-to-noise ratio over the frequencies in the LISA window. Because the sensitivity of the LISA window starts 'bumping' on the higher-frequency side, and also because the jet source has a comparatively lower amplitude in this region and thus contributes less to the integrated signal-to-noise ratio, we consider a frequency range of 10^{-4}–2×10^{-2} Hz for LISA sensitivity to calculate the relevant quantities.

We therefore compute the suitably averaged signal-to-noise ratio for the source at about 3 Gpc. It is apparent that the signal-to-noise ratio scales linearly with the mass creation rate as follows:

$$\mathrm{SNR} = 5.19 \times \left(\frac{\dot{M}}{100\,\mathrm{M}_\odot\,\mathrm{s}^{-1}} \right). \tag{34}$$

This is also obvious from the expression for the gravitational-wave amplitude. From this expression, the minimal mass creation rate for which a source is just observable can be calculated. Here we consider this 'bare visibility' value for the signal-to-noise ratio to be 10. In this case, the mass creation rate turns out to be about $200\,\mathrm{M}_\odot\,\mathrm{s}^{-1}$.

Although it is easier to compute the signal-to-noise ratio using only the instrumental noise, a remark is in order here, because the instrumental noise in LISA below 1 mHz is dominated by the 'confusion' noise from galactic binaries. These independent unresolved sources form a stochastic background that stands above the instrumental noise. Since equation (34) only takes into account the instrumental noise in LISA, the signal-to-noise ratio as calculated above will degrade because the confusion noise will effectively raise the noise floor at low frequencies. A recent calculation has been performed by Edlund et al. (2005) of the galactic background noise which shows that the previous estimates of this noise were overestimates, and that the level of the noise is a factor of 2 or more less than was previously thought. Using this current result, we estimate that the signal-to-noise ratio given in equation (34) will be degraded by less than 10 per cent on account of the galactic confusion noise. This, then, does not affect our order-of-magnitude estimate of the signal-to-noise ratio.

The net gravitational-wave amplitude from an MCE, in the linear approximation, can be thought of as arising from the superposition of gravitational waves from individual fluid elements of the MCE. If f is the frequency of interest, coherent superposition of amplitudes occurs only from within a region $2\mathcal{L}$ of size less than $0.5\lambda = 0.5c/f$. For the LISA window ($f_1 = 10^{-4}$ to $f_2 = 2 \times 10^{-2}$) Hz, we have

$$2\mathcal{L}_1 < \frac{c}{2 \times 10^{-4}\,\mathrm{Hz}} \quad \Rightarrow \quad \mathcal{L}_1 < (2500\,\mathrm{s})\,c,$$

$$2\mathcal{L}_2 < \frac{c}{2 \times 2 \times 10^{-2}\,\mathrm{Hz}} \quad \Rightarrow \quad \mathcal{L}_2 < (12.5\,\mathrm{s})\,c;$$

that is, towards the higher frequencies the jet length limit is smaller, and towards the lower-frequencies it is larger. This means, under the linear approximation, that the gravitational-wave frequency in the LISA window will carry information about the MCE during which the jet acquires the above length limit. This length limit can be converted to a time limit from knowledge of the velocity of expansion of the jets. The corresponding time limit is

$$\left(\frac{\mathcal{L}_1}{u} - \frac{\mathcal{L}_2}{u} \right) = \left(\frac{2500c}{0.8c} - \frac{12.5c}{0.8c} \right) \mathrm{s} \simeq 3100\,\mathrm{s} \approx 52\,\mathrm{min};$$

that is, LISA observation of an MCE can look into the history from 15 s after the birth of an MCE for a duration of about 52 min. However, LISA will be able to 'see' the jets for which the mass creation rate is at least $\dot{M} = 200\,\mathrm{M}_\odot\,\mathrm{s}^{-1}$. This mass creation rate is then converted to a single jet mass window of $(1.56 \times 10^3, 3.13 \times 10^5)\,\mathrm{M}_\odot\,\mathrm{s}^{-1}$.

6 OBSERVATION OF MCES BY A LIGO-TYPE DETECTOR

For the LIGO-type detectors, Wiener optimal filters $q(t)$ are used. These filters are defined by their Fourier transform (Thorne 1987; Schutz 1991) as

$$\tilde{q}(f) = k \frac{\tilde{h}(f)}{S_{\rm n}(f)}, \tag{35}$$

where $S_{\rm n}(f)$ is the power spectral density of the noise in the detector and k is a normalization constant. For a laser interferometric detector of advance LIGO type, $S_{\rm n}(f)$ is given in the following form:

$$S_{\rm n}(f) = \begin{cases} \infty, & f < 10\,\mathrm{Hz}, \\ S_0 \left\{ \left(\dfrac{f_0}{f} \right)^4 + 2 \left[1 + \left(\dfrac{f^2}{f_0{}^2} \right) \right] \right\}, & f > 10\,\mathrm{Hz}, \end{cases} \tag{36}$$

where $S_0 = 3 \times 10^{-48}\,\mathrm{Hz}^{-1}$ and $f_0 = 70$ Hz (Cutler & Flanagan 1994[1]). The amount of detector noise determines the strength of the weakest detectable signal. For a perfect frequency matching of the filters with the signal, the cross-correlation between the detector outputs and the filter leads to a signal-to-noise ratio

$$\mathrm{SNR} = \left[2\int_0^\infty \frac{|\bar{h}(f)|^2}{S_n(f)}\,\mathrm{d}f\right]^{1/2}. \tag{37}$$

We assume that the present detector is uniformly sensitive in the frequency band $f_\mathrm{l} = 10$ Hz to $f_\mathrm{u} = 1000$ Hz and is blind everywhere outside it. Then equation (16) reduces to the form

$$\mathrm{SNR} = \frac{\sqrt{2}G\dot{M}u^2 f_0}{3c^4\pi^2 R S_0{}^{1/2}}\left[\int_{f_\mathrm{l}}^{f_\mathrm{u}} \frac{\mathrm{d}f}{(2f^6 + 2f_0^2 f^4 + f_0^6)}\right]^{1/2}. \tag{38}$$

Computing the integral numerically, we obtain

$$\mathrm{SNR} \sim \frac{G\dot{M}u^2}{c^4\pi^2 R}(3.76 \times 10^{20})\,\mathrm{Hz}^{-1}. \tag{39}$$

On choosing the following values,

$$\begin{aligned} r &= \frac{c}{2H_0} \equiv \text{half the Hubble distance (for } h_0 = 0.65),\\ u &= \frac{8c}{10} \equiv \text{ eight-tenths of the velocity of light,}\\ \dot{M} &= \frac{\kappa}{\tau}\,\mathrm{M}_\odot, \text{ where } \kappa \text{ is a constant and } \tau \text{ is the proper}\\ &\quad \text{time measured in seconds,} \end{aligned} \tag{40}$$

we obtain the following result:

$$\begin{aligned} \mathrm{SNR} &\sim 5.3 \times 10^{-4}\left(\frac{\dot{M}}{\mathrm{M}_\odot}\right)\\ &= 5.3 \times 10^{-4}\left(\frac{\kappa}{\tau}\right). \end{aligned} \tag{41}$$

We next relate such values to actual situations, for which we need to go back to the astrophysics of an MCE. We return to Section 2 to discuss further details of the typical MCE. The *C* field obeys the wave equation with sources in the world points where particle creation takes place (Hoyle et al. 1995a). So when matter is created at a point, the negative-energy *C* field tends to escape outwards more efficiently than the matter created, which has non-zero rest-mass. Thus initially the mass created adds to the existing massive object. It is this tendency that leads to the build-up of massive concentrations of matter such as found in the nuclei of galaxies. However, as the central mass grows and its gravitational field increases in strength, the free escape of the *C*-field quanta is inhibited, and this leads to a concentration of the field in the object. Since the field has negative stress, the interior of the collapsed object tends to become unstable. With sufficient accumulation of *C*-field strength, it may break up and cause some pieces to be thrown out with great speed. It was this scenario that was envisaged in Section 2, and, as stated there, if the collapsed object is a near-Kerr black hole, it will eject material along the axis. Although the material is coming out of a region of high gravitational redshift, its ejection speed can be even more dominant and allow it to come out with high speed. The situation is somewhat like the classical white hole (see for example Narlikar, Apparao & Dadhich 1974), except that in this case the *C* field is the driving agent, preventing the outgoing material from being swamped by the relative inward motion of the surrounding material, thus overcoming an objection to white holes envisaged by Eardley (1974). In such a case, the early expansion is very rapid, with the external observer receiving radiation that is highly blueshifted. The blueshift does not last long, however, and the expansion subsequently slows down.

Finally, we address an important issue relating to the expected frequency of these events. If mass concentrations in the universe are too frequent, then there may be a confusion background of such events, making it impossible to detect single sources. If we confine our attention to radio sources, we may estimate their total number out to 3 Gpc to be about a few times 10^8; this is the distance to which the signal-to-noise ratio ∼10 or greater on average. This number can be arrived at by taking one radio galaxy per 100 Mpc^3 or one per few hundred Mpc^3. A characteristic time-scale for a source is $\sim 10^8$ yr. As we have seen, however, the present specifications of the LISA detector allow observation of a source for a typical time-window of $\sim 3 \times 10^3$ s. The chance of observing a given source is therefore $3 \times 10^3\,\mathrm{s}/10^8\,\mathrm{yr} \sim 10^{-12}$. The total probability is therefore a few times $10^8 \times 10^{-12} \sim$ a few times 10^{-4}. Thus the observation of MCE in a characteristic time-window is a fairly rare one and certainly not one to generate noise. Given that there are $3 \times 10^7/3 \times 10^3 \sim 10^4$ such windows per year, we expect one to a few positive detections by LISA over a year. We would like to point out here that these numbers are only approximate, because a detailed calculation should take into account effects such as the non-Euclidean nature of the specific cosmological model, etc. Nevertheless, the numbers indicate that MCEs could be detected by LISA during its mission period.

7 CONCLUSIONS

Gravitational waves could be generated in a chain of endless mini-bangs if there is a small anisotropy present in the process. An anisotropic MCE is the biggest source of gravitational waves. The calculations we performed here show that a laser interferometric detector of the LISA type can be used to detect through a window of low-frequency range 10^{-4} Hz to 2×10^{-2} Hz for a duration of about 52 min. In this duration, LISA will be able see 'jets' for which the mass creation rate is at least $200\,\mathrm{M}_\odot\,\mathrm{s}^{-1}$. On the other hand, a laser interferometric detector of the advance LIGO type can be used to detect the MCEs, which opens its window of high-frequency range 10 to 10^3 Hz for a very short duration of the order of 10^{-2} s, and in this duration it observes 'jets' for which the mass creation rate is $2 \times 10^4\,\mathrm{M}_\odot\,\mathrm{s}^{-1}$. It appears from this elementary analysis that the LISA detector is well suited to detecting MCEs through their gravitational waves, while the LIGO may have a less sensitive, marginal role to play.

ACKNOWLEDGMENTS

BPS and SKB acknowledge facilities provided by IUCAA.

REFERENCES

Armstrong J. W., Eastabrook F. B., Tinto M., 1999, ApJ, 527, 814
Bender P. et al., 2000, LISA: A Cornerstone Mission for the Observation of Gravitational Waves. System and Technology Study Report ESA-SCI, 11
Bondi H., Gold T., 1948, MNRAS, 108, 252
Cutler C., Flanagan E. E., 1994, Phys. Rev. D, 49, 2658
Das Gupta P., Narlikar J. V., 1993, MNRAS, 264, 489
Dhurandhar S. V., Nayak K. R., Vinet J.-Y., 2002, Phys. Rev. D, 65, 102002

[1] Because we are only interested in the order-of-magnitude estimate, this noise curve suffices.

Eardley D. M., 1974, preprint
Eastabrook F. B., Tinto M., Armstrong J. W., 2000, Phys. Rev. D, 62, 042002
Edlund J. A., Tinto M., Krolak A., Nelemans G., 2005, Phys. Rev. D, 71, 122003
Hoyle F., 1948, MNRAS, 108, 372
Hoyle F., Burbidge G., Narlikar J. V., 1993, ApJ, 410, 437
Hoyle F., Burbidge G., Narlikar J. V., 1994a, MNRAS, 267, 1007
Hoyle F., Burbidge G., Narlikar J. V., 1994b, A&A, 289, 729
Hoyle F., Burbidge G., Narlikar J. V., 1995, Proc. R. Soc. A, 448, 191
Hoyle F., Burbidge G., Narlikar J. V., 2000, A Different Approach to Cosmology. Cambridge Univ. Press, Cambridge
Misner C. W., Thorne K., Wheeler J. A., 1973, Gravitation. W. H. Freeman and Company, New York
Narlikar J. V., Padmanabhan T., 2001, ARA&A, 39, 211
Narlikar J. V., Apparao K. M. V., Dadhich N. K., 1974, Nat, 251, 590
Narlikar J. V., Vishwakarma R. G., Burbidge G., 2002, PASP, 114, 1092
Nayak K., Rajesh Dhurandhar S. V., Pai A., Vinet J-Y., 2003, Phys. Rev. D, 68, 122001
Sachs R., Narlikar J. V., Hoyle F., 1996, A&A, 313, 703
Schutz B. F., 1991, in Blair D. G., ed., The Detection of Gravitational Waves. Cambridge Univ. Press, Cambridge, p. 406
Thorne K. S., 1987, in Hawking S., Israel W., eds, 300 Years of Gravitation. Cambridge Univ. Press, Cambridge, p. 330
Tinto M., Armstrong J. W., 1999, Phys. Rev. D, 59, 102003

This paper has been typeset from a TEX/LATEX file prepared by the author.